Proceedings of the 7th International Symposium on Cavitation
CAV2009
August 17-22, 2009, Ann Arbor, Michigan, USA

CAV2009 – Paper No. 114

Blade Section Design of Marine Propellers with Maximum Inception Speed

Zhibo Zeng
China Ship Scientific Research Center
Wuxi 214082, China

Gert Kuiper
Consultant
Wageningen, The Netherlands

ABSTRACT

Kuiper and Jessup (1993)) developed a design method for propellers in a wake. This method is based on the use of the Eppler foil design method. The optimized section is transformed into the three-dimensional propeller flow using the approach of the effective blade sections. Effective blade sections are two-dimensional sections in two-dimensional flow which have the same chordwise loading distribution as the three-dimensional blade sections of a propeller.

However, the design procedure is laborious in two aspects: finding an optimum blade section using the Eppler program requires much skill of the designer, and transforming the two-dimensional blade section into a propeller blade section in three-dimensional flow is complex. In this paper, these two problems are dealt with. A blade section design procedure is presented using an optimization technique and an alternative procedure for the effective blade section is developed using a lifting surface design method. To validate the method a benchmark model of a naval ship was used. This benchmark model was extended by new appendices and a reference propeller, designed using conventional design methods. This reference propeller was optimized using the new design procedure and model tests were carried out Special attention was given to the data of the model and the reference propeller, to make the configuration suitable for RANS calculations.

INTRODUCTION

Cavitation is a key subject of ship propeller design. In many cases, such as for naval ships, it is necessary to delay cavitation up to the highest possible ship speed.

Traditionally the margin against cavitation is increased by increasing the blade area. However, this leads to thin and wide sections which reduces the ability of the blades to adapt to wake variations without cavitation. Furthermore, increasing the blade area reduces the propeller efficiency.

To move cavitation inception to the highest possible ship speed it is necessary to control the pressure distribution on the propeller blades at all blade positions in a wake. This requires optimization of the blade sections at all of angles of attack that are encountered during a propeller revolution. The range in which a profile or a blade section can operate without cavitation is expressed in graphical form by a “cavitation bucket”.

Giving up foil design based on a linearized theoretical basis, Shen[1] founded a new class of blade sections of marine propeller utilizing Eppler’s aerofoil design method [2]. Efforts have been made to enlarge the cavitation bucket of foils to increase the cavitation inception speed of a propeller. Bailar at al (1992） first optimized a blade section using the Eppler method and then used this blade section in propeller design. The prototype testing was carried out in 1994, which validated the theoretical design method[3,4]. Kuiper and Jessup (1993) [5] developed an integrated non-cavitating propeller design method for the unsteady condition, and the method was validated by model tests and full-scale trials. Dang,et al.(1998)[6] designed the rear wing of hydrofoil boat and propellers of underwater vessels using the Eppler method, and the test results showed that the designed new section delayed cavitation inception. The design experience shows that the cavitation bucket making use of new sections is 30% wider than that of the NACA profiles in the same design conditions. Zhou Weixin (2002)[7] also designed new blade sections and verified the results for a ship propeller. The model test results showed that the new section design method increased the cavitation inception speed of the ship.

This paper follows the design method as developed by Kuiper and Jessup[5], but improves the way the Eppler foil design method is used and follows a different and easier way to deal with the transformation of the two-dimensional effective profile into a blade section.

DESIGN PHILOSOPHY

The design cycle starts with the choice of an attainable inception speed for a given ship. This is an estimation and the

optimization cycle in the design will show if this choice was too low or too high. In the following this speed will be called the design speed.

The first step in the design cycle is the design of an initial propeller. The thrust, rotation rate, the propeller inflow (wake distribution), the blade contour (which implies diameter, skew and blade area), the radial loading distribution and the rake distribution are chosen on the basis of expected or required propeller performance. These are input parameters for the present design process and they are only changed when the results of the design process need further improvement.

Initial values are chosen for the chordwise loading distribution, which may differ per radius but is generally taken the same at all radii. This distribution can be taken from "standard distributions" such as the NACA camber distributions.

The pitch and camber distribution of the initial propeller are then obtained using a lifting surface design approach. The geometry of the initial propeller is then found by adding an initial thickness distribution, which also may be taken from a NACA profile.

The hydrodynamic characteristics of this initial propeller, with a hub added, is analyzed with a surface panel method in uniform inflow. This is done to check the thrust. The lift coefficient at every radius can be obtained by integrating the pressures calculated by the surface panel code.

The unsteady performance of the initial propeller is evaluated with an unsteady panel method at the (corrected) design speed in the wake. The focus is on the minimum pressure at any the blade position. If this minimum pressure is lower than the vapor pressure, cavitation will appear, and further improvement is necessary to bring the inception speed to the design speed.

This improvement goes as follows. From the calculation with the unsteady panel method, the lift coefficients and cavitation indices with the blade position are obtained at or near the radius with the minimum pressure. This radius can be assumed to be the most critical for the inception speed. These values are used to form the operating curve at this radius.

A new blade section is then designed using the method of Eppler [2]. In this paper an optimization method is described to obtain a section with a cavitation bucket which envelopes the operating curve. If such a section is possible the optimization proceeds. If not, the assumed inception speed has been taken too high.

The resulting new blade section is separated into a camber and thickness distribution in a linearized way. Then the first step of the design cycle is entered again, but now with the new camber and thickness distribution. Instead of the initial propeller the first optimization is then found. This iteration is completed when the camber and thickness distributions converge. Generally only a few cycles are necessary.

The use of the lifting surface design code in this way is an alternative to the use of a two-dimensional effective profile and is more efficient when the propeller codes are available. Fig.1 shows a camber distribution (two-dimensional) as designed by the Eppler method from the operating curve and the camber distributions of the propeller as derived from the effective profile approach with lifting surface corrections and the present lifting surface design approach. The resulting camber distributions of both approaches are nearly the same.

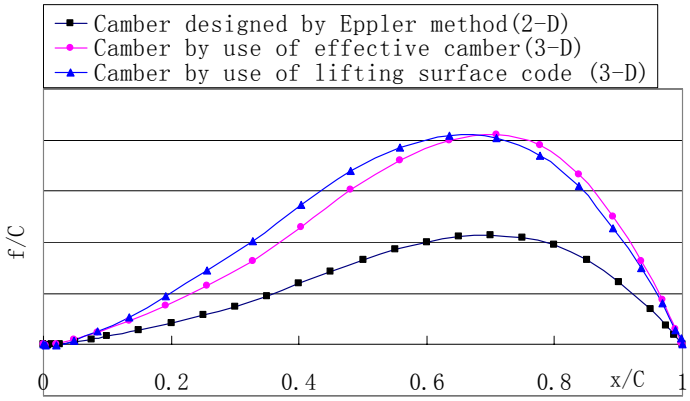

Figure 1: Comparison of different camber distributions

The minimum pressure on the newly designed propeller in the wake is checked using an unsteady panel calculation . If the minimum pressure at a radius different from the optimized radius is still lower than the vapor pressure this other radius will be optimized until the pressure on the propeller remains higher than the vapor pressure at all radii and in all blade positions. If there is a margin between the minimum pressure and the vapor pressure the inception speed can be further increased.

BLADE SECTION DESIGN OPTIMIZATION

The program of Eppler-Shen (1980)[2] is used in the new blade section design. Optimization using such a routine is difficult. A routine for automatic and convenient optimization has been developed, using the commercially available program iSIGHT, which gives the desired blade section with sufficient accuracy.

The Eppler code describes a profile by ten parameters:

$$\phi_1, \alpha_1, \alpha_2, \phi_3, \alpha_3, \phi_4, \alpha_4, \alpha_5, u, k$$

The detailed description of the input parameters can be found from Kuiper et.al(1993)[5].

The objective of the optimization is to design a section with a cavitation bucket which envelopes the operating curve(Fig.2).The cavitation bucket indicates the region where no cavitation occurs and is a property of a blade section. The operating curve has been calculated by the unsteady panel code. The optimization objective has been expressed in the three variables: $d\alpha_1$, $d\alpha_2$ and dcp. The value $d\alpha_1$ is the vertical distance between the cavitation bucket and the lowest point of the operating curve. It gives the margin against pressure side sheet cavitation. The value $d\alpha_2$ is the vertical distance between the cavitation bucket and the highest point of the operating curve. This value gives the margin against suction side sheet cavitation. Similarly the value dcp depicts the minimum horizontal distance between the operating curve and the bucket and it depicts the margin against suction side bubble cavitation.

iSIGHT uses orthogonal arrays to generate a set of designs within specified parameter ranges. This orthogonality allows for independent estimation of factor- and interaction effects from the entire set of experimental results. When there is a strong dominance of some parameters on the objectives this saves much time in the optimization. The automation of this procedure in iSIGHT allows a designer with little knowledge of orthogonal arrays to efficiently and effectively study the design space. Fig.3 shows the Pareto for the impact of the top 10 parameters on the object $d\alpha_2$ .In the Figure the blue bars represent a positive effect and the red a negative effect on the object. The top 10 parameters are not only the independent ones, such as $\alpha_1, \alpha_2, \phi_1, k, \phi_4$, but also the interaction terms, for example:'3-1' in the Figure denotes the effect of the interaction terms: ϕ_1 and α_1 on $d\alpha_2$.

In order to optimize the design variables the objectives are translated into one fitness parameter with suitable weight for each of the design objectives. A genetic algorithm(GA) optimization method is used to generate a new better population. Optimizations are processed by means of genetic operators, including crossover, mutation and selection. In the section optimization, it was enough to set population size at 10, and after about 30 generations the optimized solution was obtained. The time to optimize a section is less than 10 minutes, so it takes less than half an hour to design 3 sections for a propeller. The final generation has some individuals with optimum fitness.

The best solution for a multi-objective optimization problem is often a trade-off, so a Pareto optimum is used instead of finding only one solution. There is a series of feasible and non-dominated solutions in the Pareto. In the section optimization, there are three Paretos: $d\alpha_1$ and $d\alpha_2$; $d\alpha_1$ and dcp ; $d\alpha_2$ and dcp .Fig.4 showed the Pareto for $d\alpha_1$ and dcp. In the Figure there are all the individuals in every generation during the process of optimization in which the light blue dots are the final optimum individuals and designers can select a suitable one according to practical requirements.

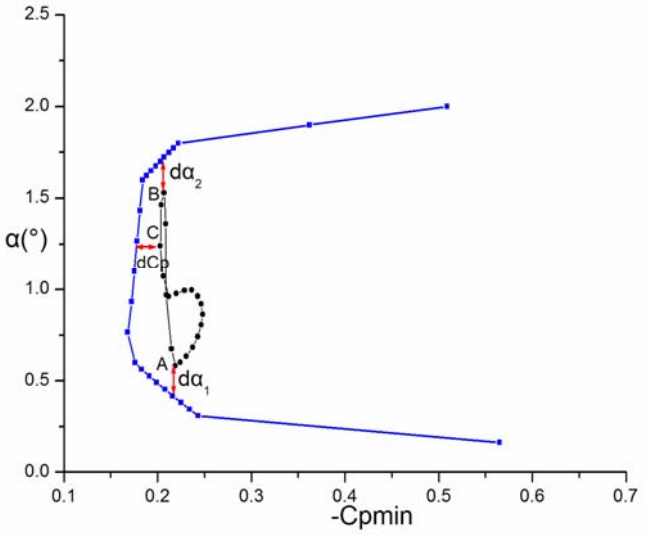

Figure 2: A typical operating curve and cavitation bucket

.

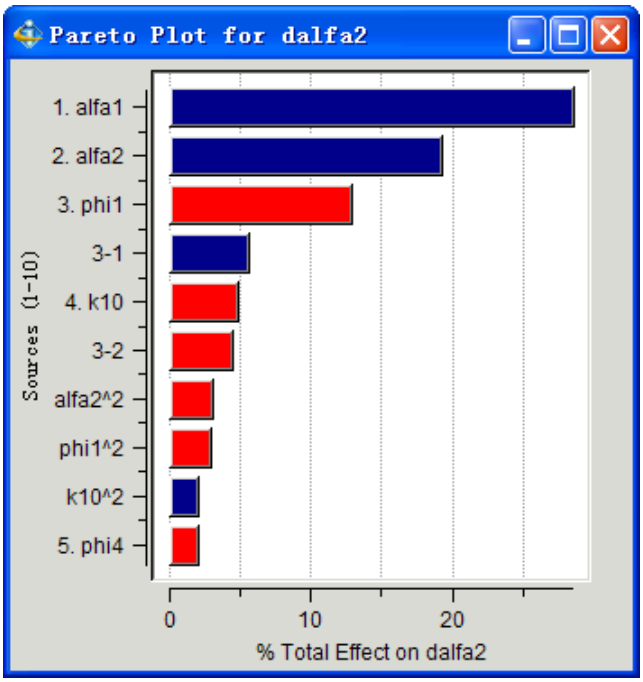

Figure 3: The Pareto for the impact of design variables on $d\alpha_2$

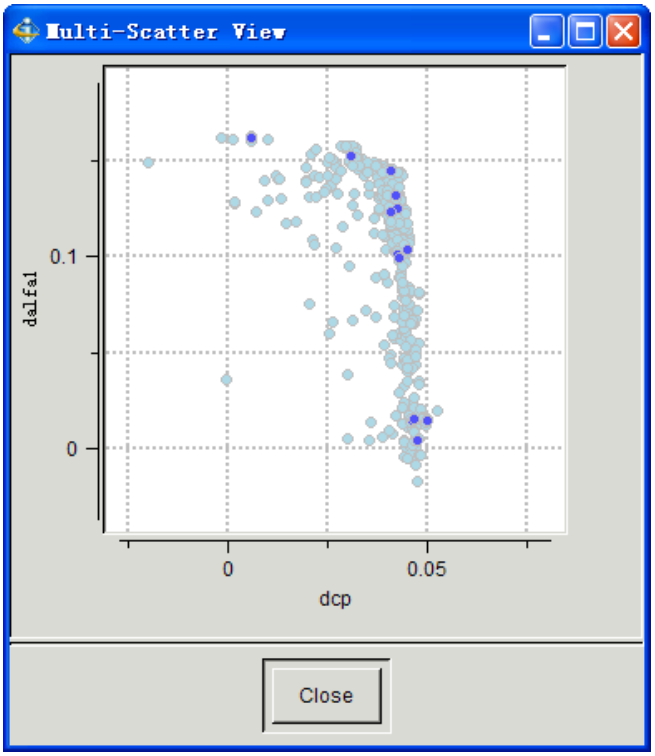

Figure 4: The Pareto: The distribution in the objective space of all the individuals

DESIGN OF A REFERENCE CASE

To apply and illustrate the method a specific twin screw frigate type ship has been used: DTMB Model 5415. This model has been used as a benchmark for flow calculations and wave calculations.[8,9,10,11]. The data of this model did not include a realistic propeller and realistic struts. Therefore a reference propeller was designed with a good cavitation behavior using a standard conventional design method. It is our aim to use this reference propeller also for the validation of RANS calculations of propellers. In this paper this reference propeller is used to optimize the inception speed of sheet and bubble cavitation.

The design of a reference propeller is carried out using standard NACA sections.

WAKE DISTRIBUTION

The three dimensional wake was obtained from RANS calculations of the appended hull with shafts and struts. The calculated axial wake has been compared with test results in the Large Cavitation Channel of CSSRC in Wuxi,China (CLCC).The waterline length of the model 5415 is 5.72m and the velocity of the channel flow is about 3.3m/s in the wake measurement. The results at 0.7R and 0.9R are shown in Figs.5-6. It can be seen that the calculated axial wake has the same distribution as the measured one, but it has a slightly deeper wake peak. The calculated three dimensional wake was used to design propellers in the paper and the accuracy was enough for the propeller design.

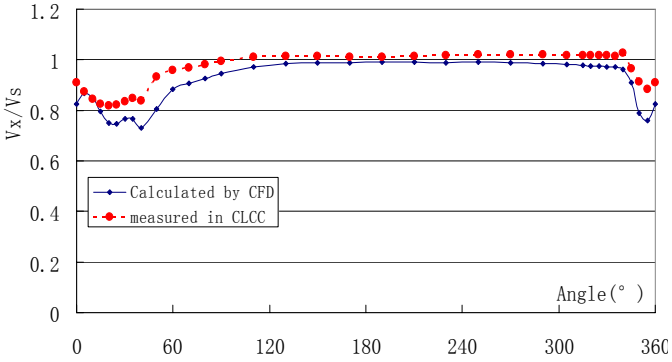

Figure 5: Comparison of the calculated and measured axial wake distribution at 0.7R

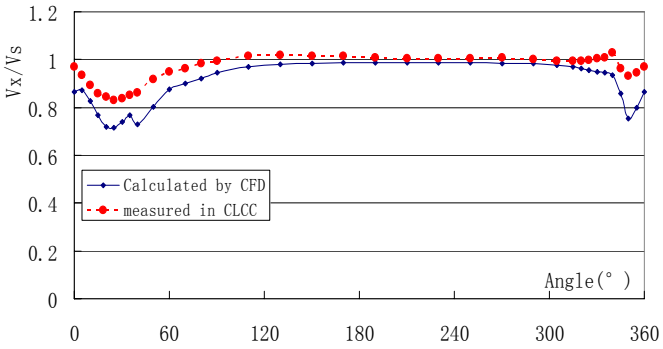

Figure 6: Comparison of the calculated and measured axial wake distribution at 0.9R

STRUT DESIGN AND ALIGNMENT

The original strut of model 5415 in the benchmark was found to be very sensitive to cavitation when initial cavitation observations at full speed were carried out in the Cavitation Channel. The cavitation index based on the flow in the channel is $1.0 \le \sigma \le 1.05$ along the struts, and the propeller loading K_T=0.20. In that condition the pressures on the struts and the flow field around the strut sections was calculated using Fluent-6.3. The propeller forces were represented by body forces, distributed according to Paterson[12].

The photo on the left of Fig.7 shows cavitation on the original inner strut. The calculated pressure is indeed lower than the vapor pressure. In many conditions the strut cavitation interfered with the cavitation on the propeller, so it was necessary to improve the strut design.

The angle of attack of the inner and outer struts (Fig.7) can be extracted from the calculations when ignoring the velocities induced by the strut. The results are shown in Figs.8~9. The inflow angle is positive anticlockwise seen from the top. It can be seen that the inflow angle is decreasing with increasing distance to the hull. The direction of inflow angle is opposite between the two struts.

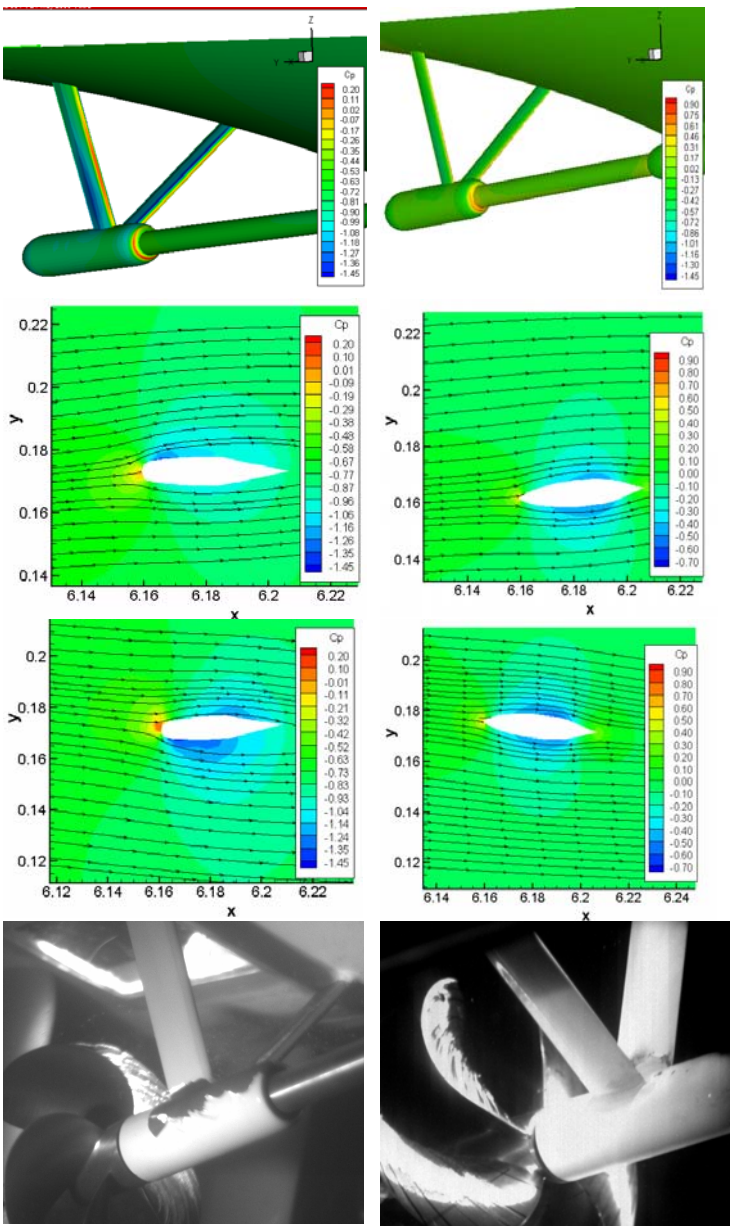

Figure 7: Calculation results and observations of the original strut (left) and on the redesigned and aligned struts (right) Top row: the starboard strut configuration; the second row: the inner strut; the third row: the outer strut; the forth row: cavitation observations.

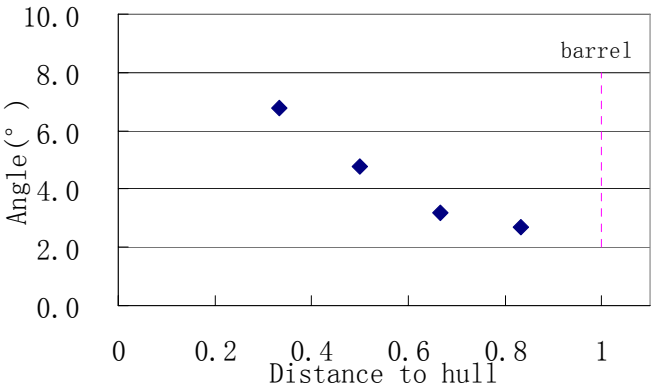

Figure 8: The inflow angle for the inner strut's sections

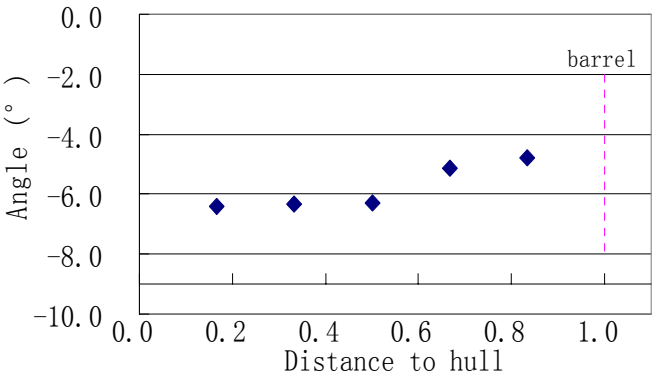

Figure 9: The inflow angle for the outer strut's sections

To arrive at an optimum strut configuration the struts should be twisted. However, for manufacturing reasons the redesigned strut has been made without twist. The new orientation of the strut has been taken as the average of the minimum and maximum angles in Figures 8 and 9. The operating curves for the strut sections are shown in Fig.10. Although most of the sections are in the bucket of the original section, there are still some exceeding the bucket of the original section and the cavitation margin is very small.. Therefore the strut section has been replaced by Profile-B from Shen[13] with the same maximum thickness as the original section. The inception margin is increased significantly, as shown in Fig10.

The alignment of the original and the new strut is shown in Fig.11. The installation angle of the inner strut is adjusted from 0 to 4.73°, the outer strut from 3.27° to -5.6° .

The pressure distribution on the new struts at the new installation angle is calculated again with propellers as the original struts by Fluent 6.3 and shown in Fig.7. The pressure coefficient is increased significantly , from -1.45 to -0.7 and there is no longer any cavitation.

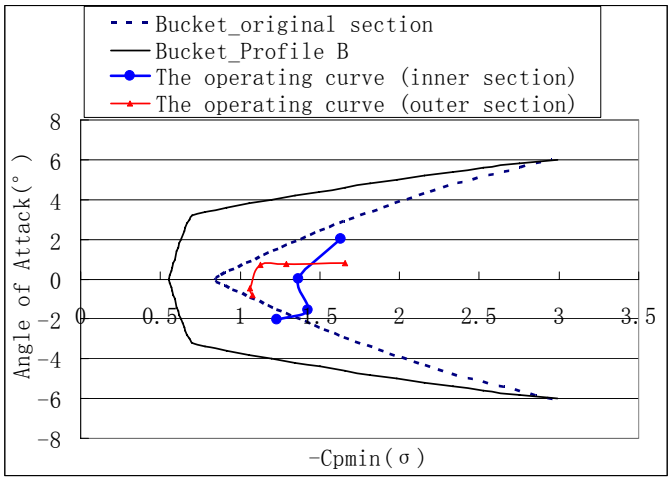

Figure 10: Buckets of the original and the new strut profiles and operating curves of the adjusted struts

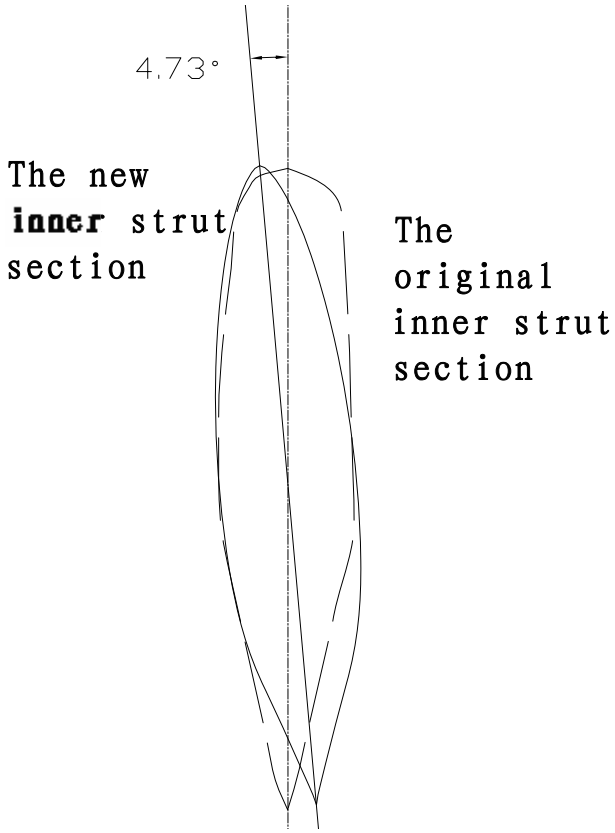

Figure 11a: The original and the new strut alignment (the inner struts on the starboard)

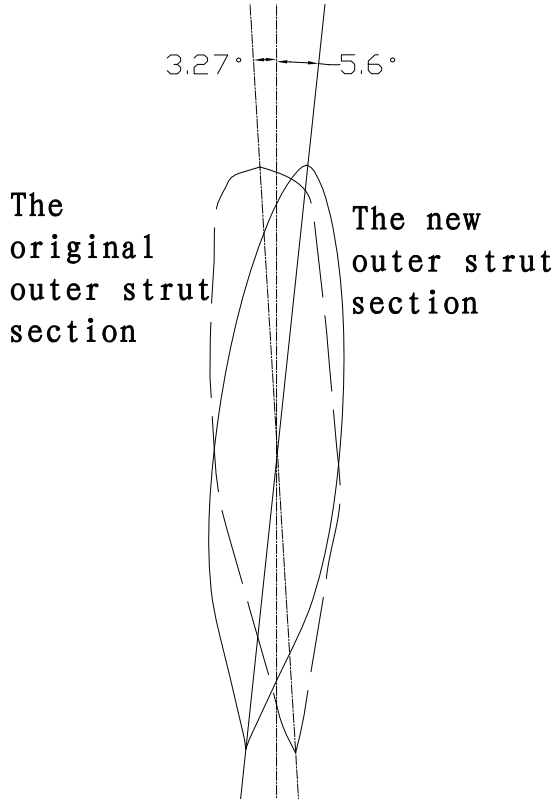

Figure 11b: The original and the new strut alignment (the outer struts on the starboard)

THE UNSTEADY PERFORMANCE OF THE REFERENCE PROPELLER

The hydrodynamic performances of the reference propeller in behind condition as measured in the CLCC is shown in Fig.12.

The design speed at which the reference propeller was to be optimized was chosen as 26kn. The thrust coefficient K_T at the design speed was 0.186 and the cavitation index at 0.9R ($\sigma_{0.9R} = \dfrac{p - p_v}{0.5\rho(0.9\pi nD)^2}$, p is the pressure at 0.9R in the top position) was 0.192.

The unsteady performance of the reference propeller in the wake at this speed was calculated using an unsteady panel method. The cavitation index and the calculated minimum pressure coefficient at 0.8R are shown in Fig.13. The minimum pressure coefficient is lower than the cavitation index in the blade positions from the top until 50 degrees beyond the top .

These calculated results were validated by model test in the CLCC. Fig14 shows a high speed observation of the reference propeller model. Sheet cavitation occurs from the leading edge on the suction side between 0.6R and 0.9R at a blade position of 36° . The observations confirmed the blade positions in which cavitation was present.

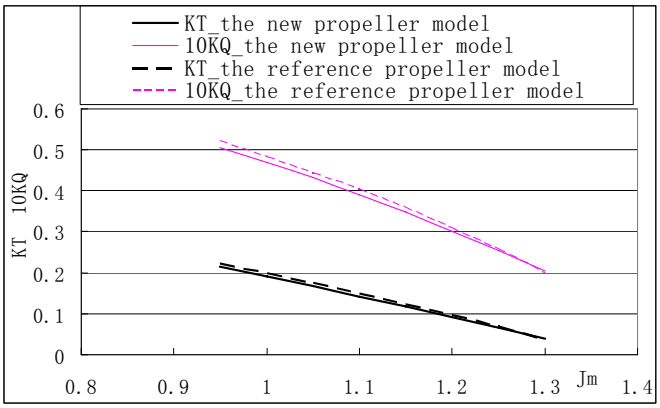

Figure 12: Measured hydrodynamic performance of the reference propeller model and of the new propeller with optimized sections in behind condition.

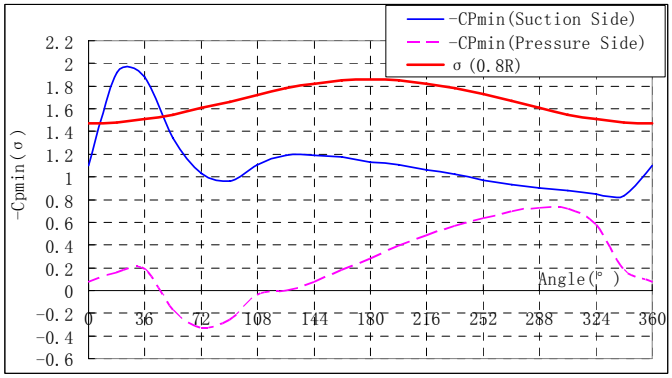

Figure 13: Cavitation index and the minimum pressure coefficient of the reference propeller(design speed,0.8R)

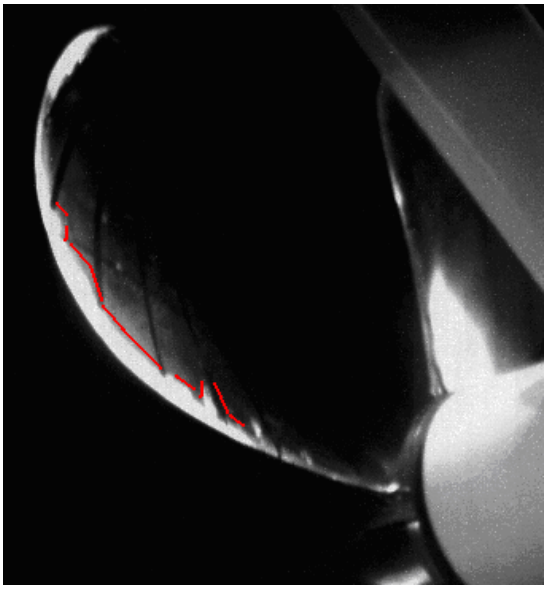

Figure 14: High speed observation on the reference propeller model at the design speed of 26knots in a blade position of 36 degrees. (the cavitation extent is enhanced)

REDESIGN FOR MAXIMUM INCEPTION SPEED

NEW BLADE SECTIONS

According to the unsteady performance of the reference propeller cavitation occurred at the design speed of 26kn. A section optimization was therefore carried out to maximize the inception of the propeller. Three blade section 0.6R,0.8R and 0.9R were selected to be optimized. Their operating curves calculated by an unsteady panel code of the reference propeller at the design (inception) speed of 26kn and at full speed of 30 kn are shown in Figs15 to 17.

The new section design optimization for the three radii were carried out as described in this paper. By maximizing the margins against sheet cavitation and bubble cavitation on the suction side and sheet cavitation on the pressure side ,the optimized buckets are obtained. The results are shown in Figs.15 to 17. They all have four "cornerpoints" which enlarges the bucket width. The buckets envelope the operating curves at the design speed with some margin. For reasons of fairing of the propeller blade it is important to keep the three optimized sections similar shape.

The new 2-D sections are shown in Fig.18. They show a similar thickness and camber distribution. The maximum thickness is moved towards the leading edge increasing the margins against sheet cavitation on both pressure and suction side. The camber is moved towards the trailing edge, moving the loading towards the trailing edge.

THE NEW PROPELLER DESIGN WITH OPTIMIZED BLADE SECTIONS

The reference propeller and the strut design is also meant to be a basis for future calculations and optimizations. The details of this design are available from the first author. The waterline length of the ship model is 6.65 and the diameter of the reference propeller model is 25cm.

The new propeller is designed by lifting surface method in the same condition as the reference one: a ship speed of 32kn and a thrust coefficient of 0.21. The only part that is changed is the chordwise loading distribution at each radius as shown in Fig.19. The loading distributions for 0.6R, 0.8R and 0.9R in Figure 19 come from the pressure difference on the new 2-D sections at their design lift coefficients. The design lift coefficient at every radius is the same as the reference propeller and is calculated by integrating the pressure from steady panel code at the corresponding radius. These loading distributions have the same shape with the main loading aft. It is not difficult to interpolate and extrapolate these loading distributions to other radii. With these chordwise load distributions, the new propeller was designed using a lifting surface design code (in uniform inflow) .

The new propeller has a new radial distribution of pitch and maximum camber. The thickness distribution of the blade can be obtained by interpolation and extrapolation from 0.6R, 0.8R and 0.9R. Fig.20 shows the radial thickness distribution of the new propeller and the reference propeller. The new thickness is larger which makes the blade section less sensitive to inflow variations in the wake. The blade contour of the reference propeller is maintained.

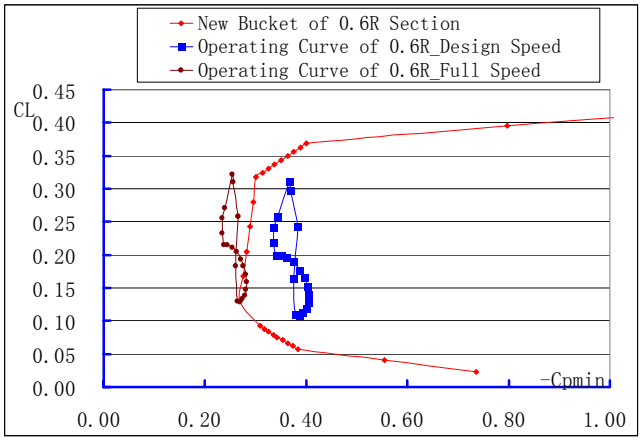

Figure 15 Optimized bucket and operating curves at 0.6R

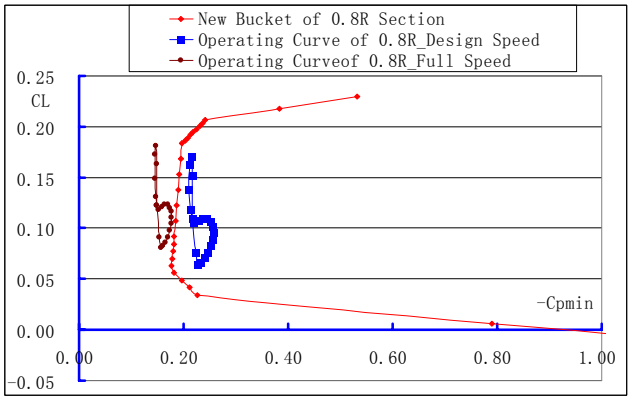

Figure 16: Optimized bucket and operating curves at 0.8R

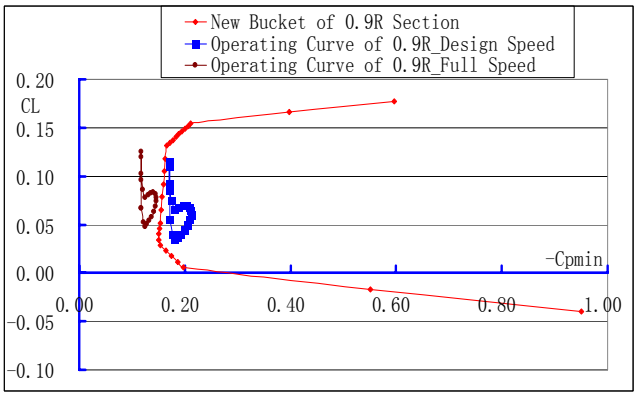

Figure 17: Optimized bucket and operating curves at 0.9R

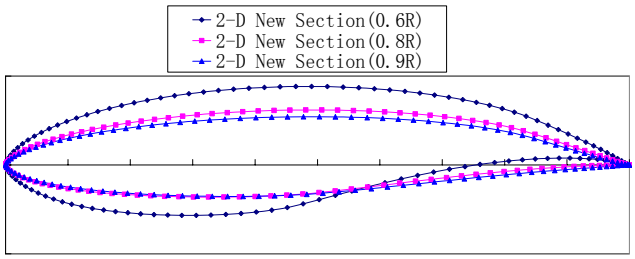

Figure 18: Optimized 2-D sections at 0.6R,0.8R and 0.9R

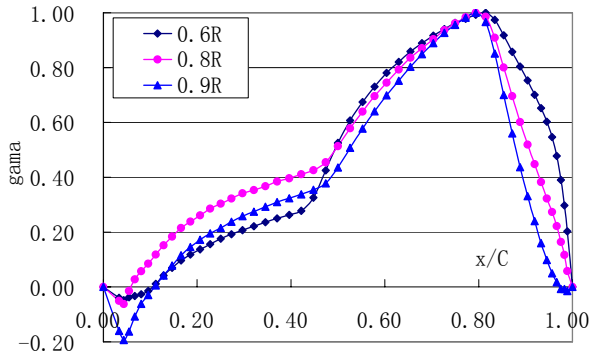

Figure 19: Chordwise load distribution of the new propeller

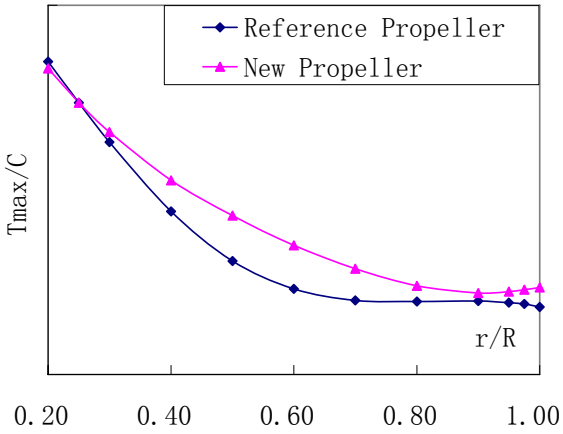

Figure 20: Radial distribution of the maximum thickness of the reference propeller and the new propeller

In general the pitch of the new propeller is decreased and the maximum camber is increased, because the zero lift angle of the new section is larger than the standard NACA section of the reference propeller.

THE UNSTEADY PERFORMANCE OF THE NEW PROPELLER

The unsteady performance of the new propeller was calculated in the same way as for the reference propeller using an unsteady panel code. Fig.21 shows the cavitation index and the calculated minimum pressure coefficient at the design speed (26 knots) on any blade position at 0.8R. Compared to the reference propeller, the minimum pressure is higher than the vapour pressure in all blade positions and thus no cavitation is expected to occur.

Figure 12 gives the hydrodynamic performance in behind condition of the new propeller. The K_T and K_Q values both are slightly lower than those of the reference propeller. The difference is very small and the new propeller has the same hydrodynamic performance.

The inception performance of the new propeller was confirmed in model tests in the CLCC. Figure 22 is in the same condition and blade position as Fig.14 and shows that there is no sheet cavitation from 0.6R to 0.9R on the blade of the new propeller at the inception design speed.

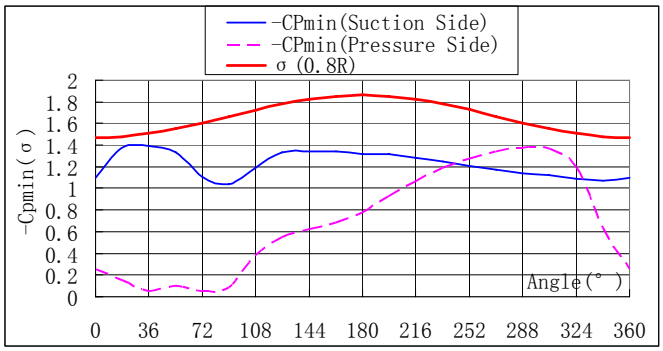

Figure21: Cavitation index and the minimum pressure coefficient of the new propeller(design speed,0.8R)

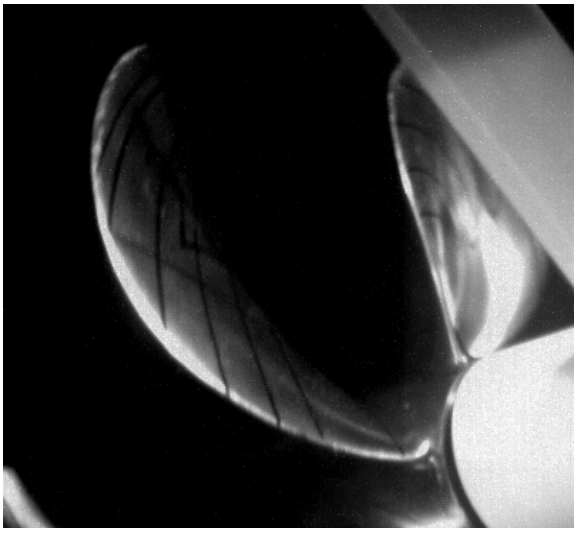

Figure 22: High speed observations on the new propeller model at design speed

CAVITATION BEHAVIOR OF THE REFERENCE PROPELLER AND NEW PROPELLER

Extensive cavitation observations and calculations heve been made on the reference propeller and on several optimized propellers. This work is ongoing. Some remarks about the cavitation observations of the new propeller with maximum inception speed can be made already.

When the cavitation appears, the cavitation reflects the calculated pressure distribution, as shown in Fig.23 at a speed of 30kn. In this Figure the pressure distribution at 0.8R is calculated by the unsteady panel code in 54° blade position, and the photo shows the corresponding cavitation from high speed observations. For the reference propeller there is a calculated pressure peak near the leading edge and the pressure coefficient is lower than the vapor pressure up to 65 percent of the chord This leads to extensive sheet cavitation, which is consistent with the picture. For the new propeller, the pressure is lower than vapor pressure from about 20 percent of the chord to 80 percent. This leads to bubble cavitation, as is also shown in the picture.

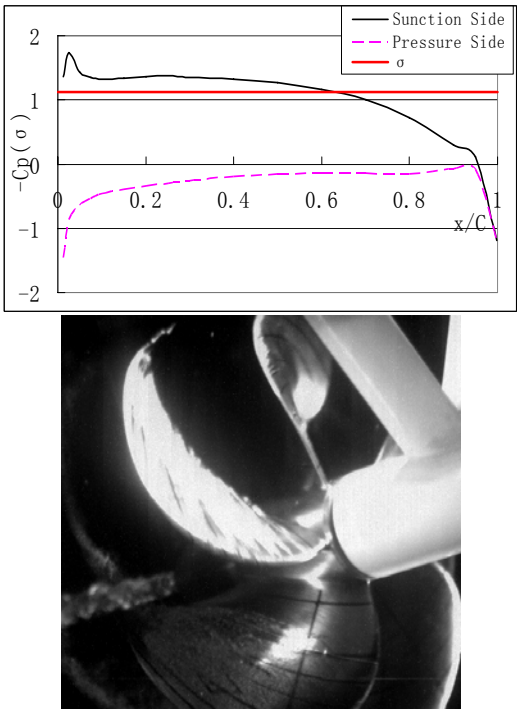

Figure 23a: Comparison of the cavitation and the calculated pressure distribution on the reference propeller; above: the pressure distribution at 0.8R; below: the high speed observation.

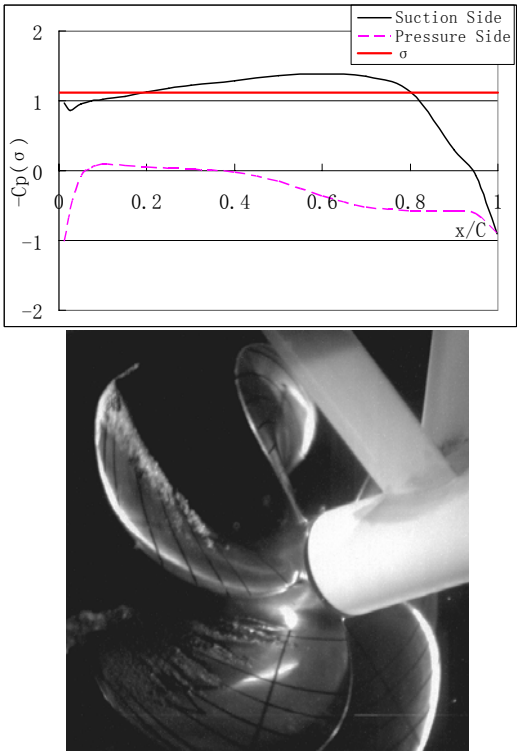

Figure 23b: Comparison of the cavitation and the calculated pressure distribution on the new propeller; above: the pressure distribution at 0.8R; below: the high speed observation)

The tests were carried out in the CLCC, with a velocity in the test section of about 6 m/s. The diameter of the model propeller was 25 cm. The rotation rate in the design condition was 1600 rpm, which leads to a sectional Reynolds number at 0.7R of 1.35 million. Earlier tests at a Reynlds number of 0.9 million showed that the sheet cavitation at the reference propeller was very incidental. A sheet was formed at highly different blade positions which gave the observations with stroboscopic illumination a very flashy appearance. This was clearly due to scale effects on inception, which means that inception occurred at local pressures far below the equilibrium vapor pressure. Also on the reference propeller in the present tests these phenomena were observed. To reduce these scale effects leading edge roughness has been applied on both the reference propeller and the new propeller with optimized blade sections. Application of leading edge roughness in the CLCC was necessary up to unexpectedly high Reynolds numbers. It is suspected that the low nuclei content of the tunnel plays a role. It seems as if a minimum amount of nuclei is still necessary. These indications are also found in the Depressurized Towing Tank at Marin at lower Reynolds numbers. This has to be investigated further.

Inception measurements were also carried out for both the reference propeller and the new propeller with optimized blade sections. This revealed another source of inaccuracy: the determination of inception on roughness elements. When inception was called in the traditional way when the first trace of cavitation was observed, the inception curves of both propellers were exactly the same, although the cavitation inception of limited cavitation was very different. The inception criterion has to be developed further. Possibly inception has to be called when the spot on the roughness elements begins to grow and becomes elongated. This will be investigated further.

The pressure distribution on the new propeller at inception is very flat on the suction side. As a result the sheet cavity will be very long and extended cavitation will occur. When the propeller blade moves out of the wake peak the cavitation will become bubble cavitation. This process was observed on the new propeller. The bubbly cavitation is quite thin and stable, without a cloudy implosion. It is therefore not expected to be erosive. Further investigations in the dynamics of very thin sheet/bubble cavities, of which the extent varies rapidly, are still necessary to assess the erosivity of this type of cavitation.

CONCLUSIONS

The design technique using new blade sections to optimize inception speed is set up in CSSRC. The paper shows the efficiency and convergence of the method. Preliminary data of a benchmark model and propeller are given. The following conclusions have been reached:

1. The optimization technique which has been developed, using a genetic algorithm to integrate the program of Eppler-Shen, makes this technique more accessible and convenient. It saves a lot of time for designers.

2. The alternative procedure for the effective blade section using a lifting surface design method makes the incorporation of 2-D sections into 3-D propeller blade sections efficient. This is especially the case when several different sections at different radii are optimized simultaneously.

3. The configuration of model 5415 with the improved struts and with the reference propeller is very useful as a basis for the validation of calculations with a RANS code.

4. Preliminary experimental results confirm that the inception behaviour of the optimized propeller is significantly improved.

5. The pressure distribution calculated by an unsteady panel code is consistent with the cavitation appearance from high speed observations, but the cavitation on a propeller with maximum inception speed is a very thin sheet with transition to bubble cavitation. Its properties have to be investigated further.

6. Application of leading edge roughness is necessary on the optimized propeller, but also on the reference propeller, up to unexpectedly high Reynolds numbers. The role of nuclei and of the tunnel have to be investigated further.

7. The determination of the inception bucket when leading edge roughness is applied requires a new definition of inception.

ACKNOWLEGEMENTS

This work was carried out in CSSRC. The authors would like to thank for support of the design group, the CFD group, the model manufacture group and the test group. Sincere thanks are extended to Prof. Shitang Dong and Prof. Denghai Tang for their continuous support. The authors wishes to express their gratitude to Prof. Weixin Zhou and Dr Xiaolong Liu for their valuable discussions.

REFERENCES

[1] Shen,Y..T., Eppler,R., 1981, “Wing Sections for Hydrofiles Part 2, Nonsymmetric Profiles”, *Journal of Ship Research*, Vol.25, No.3.

[2] Eppler, R.1980,“A Computer Program for the Design and Analysis of Low-Speed Airfoil”, *NASA Technical Memorandum* 80210.

[3] Bailar J.W., .Jessup, S.D. and Shen, Y.T., 1992, “Improvement of Surface Ship Propeller Cavitation Performance Using Advanced Blade Sections,” *23rd American Towing Tank Conference*, New Orleans, USA.

[4] Jessup S., Berberich W., Remmers K., 1994, "Cavitation Performance Evaluation of Naval Surface Ship Propeller with Standard and Advanced Blade Sections,”. *20th Symposium on Naval Hydrodynamics*.

[5] Kuiper, G. & Jessup, S.D. 1993,“A propeller design method for unsteady conditions,” *Proc. of the SNAME, SNAME Centennial Meeting*, New York.

[6] Dang J., Tang, D.H., Cheng,J.D., Peng, X.X., Qin,Q and Pan,S.S., 1998,“New blade section Design and Its Application,” *Proceedings of Third International Symposium on Cavitation*, Grenoble, France.

[7] Zhou Weixin., 2002,“The design and calculation system of propellers for naval surface ships(in Chinese),”*Phd thesis* No.B2002-01-02,China Ship Scientific Research Center.

[8] Ratcliffe, T., 2000, “An Experimental and Computational Study of the Effects of Propulsion on the Free-Surface Flow Astern of Model 5415,”*23rd Symposium on Naval Hydrodynamics* , Val de Reuil, France.

[9] Stern, F., Longo,J., Penna,R., Olivieri, A., Ratcliffe,T., Coleman, H., 2000, “International Collaboration on Benchmark CFD Validation Data for Surface Combatant DTMB Model 5415,” *23rd Symposium on Naval Hydrodynamics* , Val de Reuil, France.

[10] C.Burg, K.Sreenivas, D.Hyams, and B.Mitchell, 2002, “Unstructured Nonlinear Free Surface Simulations for the Fully-Appended DTMB Model 5415 Series Hull Including Rotating Propulsors,”*24th Symposium on Naval Hydrodynamics*, Fukuoka, Japan.

[11] Gorski,J.J., Miller, R.W., and Coleman, R.M., 2004,“An Investigation of Propeller Inflow for Naval Surface Combatants,”*25th Symposium on Naval Hydrodynamics*, *CANADA*.

[12] Eric G. Paterson, Robert V. Wilson, and Fred Stern, 2003, “General-Purpose Parallel Unsteady RANS Ship Hydrodynamics Code: CFDSHIP-IOWA, ” *IIHR Report*, No. 432.

[13] Eppler, R., Shen, Y. T. 1979, “Wing Sections for Hydrofiles, Part 1, Symmetric Profiles”, *Journal of Ship Research* , Vol.23, No.3.